International Journal of Basic and Applied Sciences, 15 (1) (2026) 59-67

International Journal of Basic and Applied Sciences

Website: www.sciencepubco.com/index.php/IJBAS
https://doi.org/10.14419/ppzpx689
Research paper



Fast K-Means Technique for Segmentation of Dermoscopic Images

Saravana Kumar V. [1] *, Kavitha M. [2], Revatthy K. [3], Anantha Siva Prakasam [4], Bavya S [5]

[1] *Galgotias University, Greater Noida, Uttar Pradesh, India*
[2] *S A Engineering College, AVADI, Chennai, Tamilnadu, India*
[3] *New Horizon College of Engineering, Bengaluru, Karnataka, India*
[4] *Rajalakshmi Engineering College, Chennai, Tamilnadu, India*
[5] *CGI, Chennai, Tamilnadu, India*
**Corresponding author E-mail: drsaravanakavi@gmail.com*

Abstract

Skin cancer remains one of the hazardous cancers diagnoses each year and accounts for more than 50%. When detected at its early stage, standard and cost-effective therapies can treat it successfully - classifying skin sores carefully is key to automating early end systems and mitigating risk factors. Melanoma can provide both shape features and areas of desire for surface examination. Unfortunately, its prevalence can be both unpredictable and lethal, leading to multiple times more passes than all other skin cancers combined. The proposed method demonstrates about the Fast K-Means clustering technique. It can be applied on the dermoscopic skin lesion images which can convert into L*u*v. This approach is then compared with the outcomes of K-Means and Fuzzy C-Means. Evaluation has carried outs includes number of pixels and time complexity analysis. Crystal clear, the proposed method is obviously segmented the lesion and display any visible lesions or spots on them.

Keywords: *Fast K-Means; K-Means, Segmentation; Skin Lesion; Melanoma.*

1. Introduction

There have been significant achievements in conventional remote medical care across the globe and particularly within developing nations; however, these activities have raised serious ethical concerns that include significant payments made directly to associated telemedicine providers as well as non-consensual therapeutic techniques being implemented without proper consent being sought from patients. Skin cancer is among the primary causes, accounting for half of all new malignancies each year. When detected early enough, fundamental and financial therapy are usually effective ways of curing this form of cancer; when automated early end procedures are utilized correctly. With regard to skin sore classification procedures. Melanoma stands out among skin malignancies as one of the more aggressive ones with blood loss often outpacing other forms. Melanoma is among the most lethal types of skin cancer when if not treated, and rates for recurrence among adolescents has dramatically increased over recent decades. Yet with early diagnosis rates being so promising, survival can often be improved significantly. Dermatologists understandably face an enormous time and cost burden in order to assess every patient for melanomas; thus, there must be modern ways for them to assess risk using photographs of dermoscopic injuries as measuring tools. Dermatologists could use such structures to augment their clinical exams without needing expensive and specialized equipment. One such test in using such systems involves finding skin lesions on photos displayed on screens. Common skin injury classification calculations typically rely on photographs taken using an unusual device called the dermatoscope, where brightness variations between on-screen photos and shadowing obfuscate any attempt at tracking damage in real time. This research's primary goal is to devise a method that will ultimately right and isolate skin injuries from an image data file. A key aspect of testing will involve showing variations in lighting with multi-organized lightening schemes to provide estimation. Apply the model to one image. From there, much can be learned about surface circulations from its original image - proving that each surface's uniqueness doesn't depend solely on one circulation alone. At last, using surface-based segregation computation, locations in photographs were classified either as normal skin or sores based on specialist surface circulation potentials. This classification could then be utilized in features extraction for modeling melanoma-related classifications.

There are two basic kinds of cluster analysis techniques; hierarchical and non-hierarchical (partional). Collectively, cluster analyses refer to collections of assets which share similarity in relation to one specific principle. These tools of data characterization allow a rapid temporary organization of large amounts of information into small clusters referred to as subclusters. Clusters provide an efficient method of distinguishing and organizing information with minimum effort. All information objects within one cluster share similarities that rely on one model. There are various models to use when framing information objects into clusters. Differentiated information that shares common characteristics is easily achieved with these standards. Before initiating cluster analysis, it's crucial that you select an accurate model and estimation. Computerized analysis methods offer advantages over manually-based clustering processes in terms of applying their methods

Copyright © Saravana Kumar V. et al. This is an open access article distributed under the Creative Commons Attribution License, which permits unrestricted use, distribution, and reproduction in any medium, provided the original work is properly cited.

to large amounts of data that have a common basis and being able to discover clusters more rapidly than manual partitioning processes could ever hope for. Data analysts often follow different clusters of similar information according to their personal standards, yet may not get results that match up perfectly with an algorithmic clustering solution. Clustering also delivers faster performance for even massive datasets in comparison with traditional methods of investigation. These methods are safe and stable, giving clustering experts an effective means of keeping data intact as well as deciphering its aftereffects more quickly and efficiently.

2. Literature Reviews

Digital Skin Lesion Imaging can play an essential part in developing an efficient computerized analysis system to assist physicians in accurately diagnosing skin lesions at different stages and making necessary modifications efficiently. To enhance understanding of skin cancers and early detection and photoprotective preventive measures are offered both to clinicians and common men alike. A system using intelligent design consisting of feature extraction using Wavelet Fuzzy C-Means was revealed. Social Group Optimization (SGO) was used to conduct a computerized examination of skin cancer created using preprocessing to improve segmentation, enhance colour detail and contrast and segment the tumour effectively. Convolutional Networks have long been pioneering applications to mask skin lesions. Lesion masks can be generated using U-net for segmentation and convolutional layer to aid discernment. VGGNet convolutional neural network design can be demonstrated. U-Otsu technique was integrated with new criteria to segmentation features for segmentation purposes and multi-Otsu process that detects border using active contour has also been created. ABC procedure has been utilized to establish an optimal threshold value for Melanoma detection. Perceptual color variance saliency together with Binary Morphological Analysis were employed in sorting images into categories for segregation purposes. Ant colony optimization (ACO) has long been employed for improving imaging enhancement. To maximize edge detection efficiency, ACO was implemented into K-Means methods including classic K-Means procedures with Robust K-Means methods used on skin pictures as well as functional methods that identify borders of lesion levels without use and an anatomical procedure used post processing of images.

L*u*v

As of CIE Yu'v' (1976), it aims to enhance our perception of colour variations within unit vectors by offering nonlinear color space that reverses conversions; information regarding hue is focused around its white spot color (D65 for most TVs). Furthermore, non-linear relationship for the Y* signal was designed to mirror eye logarithm response curve.

$$L^* = \begin{cases} 116\left(\frac{y}{y_m}\right)^{1/3} - 16 & \text{if } \frac{y}{y_m} > 0.008856 \\ 903.3\left(\frac{y}{y_m}\right) & \text{if } \frac{y}{y_m} \leq 0.008856 \end{cases} \quad (1)$$

$$u^* = 13(L^*)\,(u' - u'_n) \quad (2)$$

$$v^* = 13(L^*)\,(v' - v'_n) \quad (3)$$

L* is a scale that ranges from zero to one hundred in relation to luminance (Y/Yn) scales that go from 0-1; these three important polar parameters more accurately reflect human experience of seeing than Cartesian ones: Chroma, C* Hue huv and Psychometric Saturation Suv are other key ones that do so.

$$C^* = (u^{*2} + v^{*2})^{0.5}$$

$$huv = \arctan\left(\frac{v^*}{u^*}\right)$$

$$Suv = \frac{c^*}{L^*}$$

Hue can be described as an angle found across four quadrants of space.
Fast K-Means (FKM)
Method to split vectors by clustering them using batch K-means is described here. Rows represent points, while columns represent variables; output matrix includes centers of clusters. Column vector K-element D shows residual distortions as calculated using sum squared distances away from center for every cluster member.

K-means algorithm works on the principle that it measures distances between data points and centers using this formula:

$$dist\,(xk, xc) = \sqrt{(x_k - X_{ci})^T (x_k - x_{ci})^T}$$

Where, dist is defined as the distance from point "x", located at the center of a cluster to each of its original centers (X Ci).
Cluster points, known as x1, for 1=1 2...n clusters are denoted with "x1", with 1 being an individual point and the rest comprising each cluster's total sum of points referred to collectively as one cluster. A random selection from among data sources or arbitrarily can eliminate further calculations; by doing this it also becomes possible to skip steps altogether, saving time. At first, any K-Means-based clustering strategy is determined by its initial number of clusters with no guarantee that its centers will move closer towards or meet its mean point over time.
Assuming A_n is equal to I, we can lower J (, :P). This indicates that X_{ci} converges towards its position at the center of each group.

$$An = \{ x_{c1}, x_{c2}, x_{c3} \ldots\ldots x_{ci}\}$$

Where $J (x_{c1}, x_{c2}, x_{c3}, \ldots\ldots x_{ci}; P) = P\,(mini \mid x_k - x_i \mid^2)$

If S_n includes all data, the purpose of this exercise is to find an allocation within S_s that has greater probability than $P(S_n)$.
Assume the amount of data with one center represents an inert random sequence which matches with the sequential distribution sequence shown below:

$F_{xn,\ xn+1,\ \ldots\ldots\ldots xN}\ (x_n, x_{n+1}\ldots.x_N) = F_{xn+k,\ xn=1+k,\ldots\ldots xN+k}(x_n, x_{n+1},,x_N)$

For every succeeding term in an equation where F is >= N (x_{n+1} …..x_N)
Following is one of the more frequently used values: E(X) =c
Clustering can be defined as the process of decreasing the Within Cluster Sum of Squares quick stage value.

$$\min_s \sum_{i=1}^{Ci} \sum_{xj\epsilon Si} \left| |xj - \mu fa| \right| \quad (4)$$

$$\min_s \sum_{i=1}^{Ci} \sum_{xj\epsilon Si} \left| |xj - Csl| \right| \quad (5)$$

With C being the center of clusters that correspond exactly with those seen in Stage 1.
The Within-Cluster Sum Of Squares can be broken down into fast and intermediate clustering stages for easier analysis.

$$WSCC = \int_0^{ci} \min||x\text{-}c||, ||x\text{-}C||\ )\ dx + \int_{ci}^{1} \min\ (\ ||x\text{-}c||, ||x\text{-}C||\ )\ dx$$

The algorithm form of Fast K-Means is portrayed as below,
FKM Algorithm: Our input parameters include "S" = (n, c, per), J_k and J_s respectively
Extraction Methodology: S_n in Clusters.
Randomly choose S_n as your percentage value of S_n (c = 50 for example).
Calculate your desired distance change using ($J_f >= M_{fa}$). (i=1 to n).
Searching for Minimum D
Determine the number and location of each cluster on the scene.
Calculate the modified distance

$$D\ (x_k, x_c) = \sqrt{(x_k - X_{ci})^T (x_k - x_{ci})^T}$$

Utilise the entire dataset S_n
While ($Js \leq Ms_1$)
Compute the modified distance

$$D\ (x_k, x_c) = \sqrt{(x_k - X_{ci})^T (x_k - x_{ci})^T}$$

Find minimum of D
Calculate J_s
End Time

3. Proposed Technique

The demoscopic skin lesion image is taken as input, taken from authorised sources. Initially, convert this image into L*u*v. Since we are using unsupervised clustering methods, number of clusters have to assign initially. As per the ground truth results, here we define the number of clusters is 3. After feed the number of clusters, the algorithm starts to work as like of K-Means. The main difference of working is, K-Means working with centroid which placed randomly. Fast K-Means (FKM) is performed on these images be differentiated. Using an unsupervised algorithm to address clustering issues, FKM reduces sum of squared distances between points as well as cluster center. FKM in this instance uses histogram of intensities rather than raw data as its starting point, with each row constituting its initial cluster and then searching for its centre and refreshing as in traditional K-Means methods. As can be seen from Figure 1, here's the procedure;

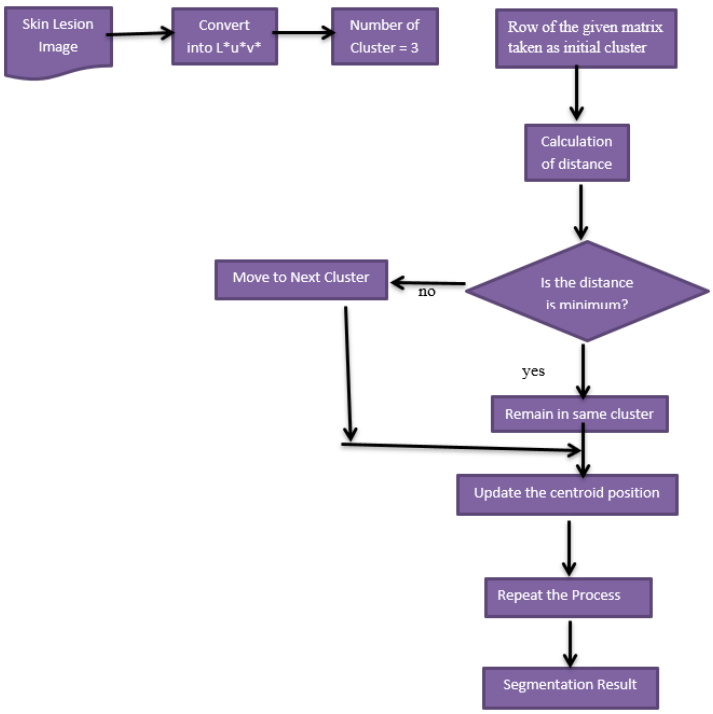


Fig. 1.1: Flow Chart for Fast K-Means Technique for Segmentation of Skin Cancer Image.

The Fast K-Means (FKM) is used to segment the dermoscopic images. This method is unsupervised algorithm to crack the renowned clustering problematic. The aims of these methods are reducing the sum of squared distances between all points and the cluster center. The results are compared with the existing clustering method namely K-Means and Fuzzy C-Means. These existing methods has been working on L*u*v images. The following figures (Figure 2.1 – 2.16) portray about the results of these unsupervised clustering methods. Figure (A) parts show the various input dermoscopic images. (B) parts show the conversion of L*u*v, whereas (C) parts shows the output generated by K-Means on L*u*v, (D) parts shows the output generated by FCM on L*u*v. The last part (E) shows that the outcomes generated by our proposed method Fast K-Means that performed on L*u*v images of various images. These works had been done using Python.

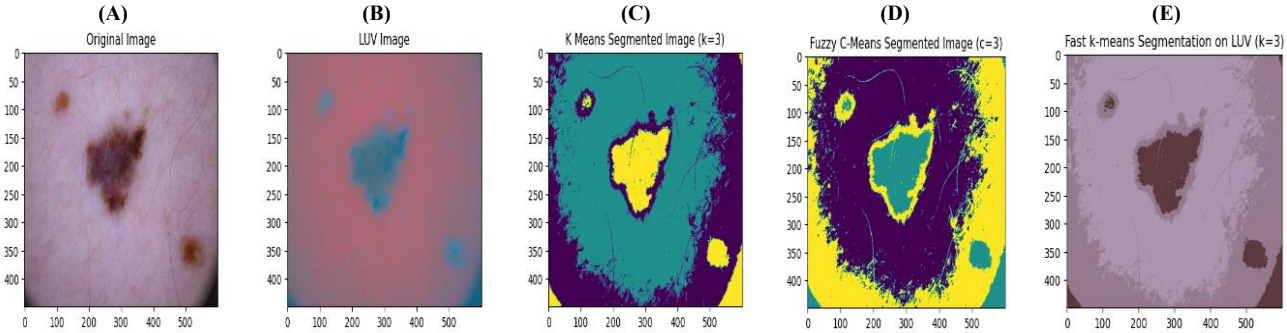


Fig. 2.1: (A) Input# Image ISIC_0024314 (B) LUV (C) K-Means (D) FCM (E) FKM.

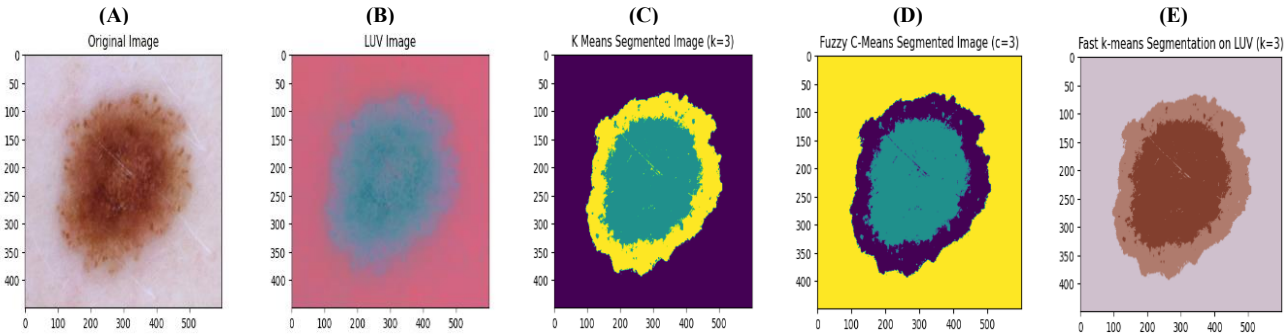


Fig. 2.2: (A) Input# Image ISIC_0024317 (B) LUV (C) K-Means (D) FCM (E) FKM.

(A) (B) (C) (D) (E)

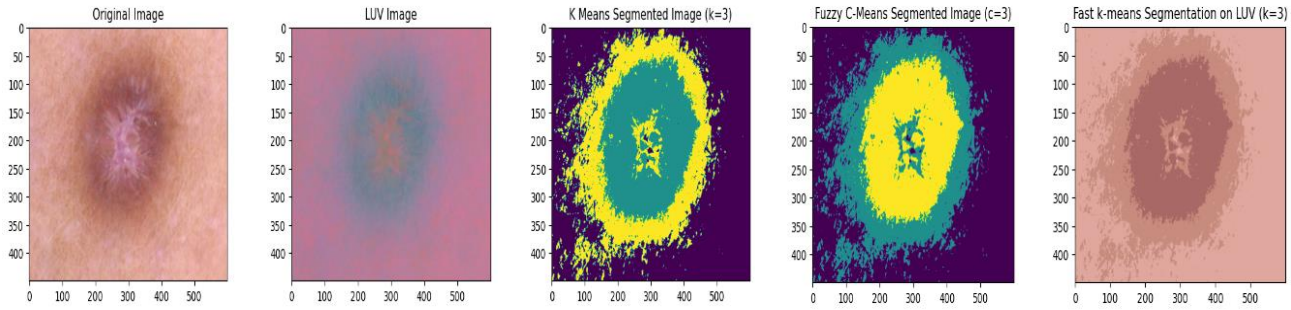


Fig. 2.3: (A) Input# Image ISIC_0024318 (B) LUV (C) K-Means (D) FCM (E) FKM.

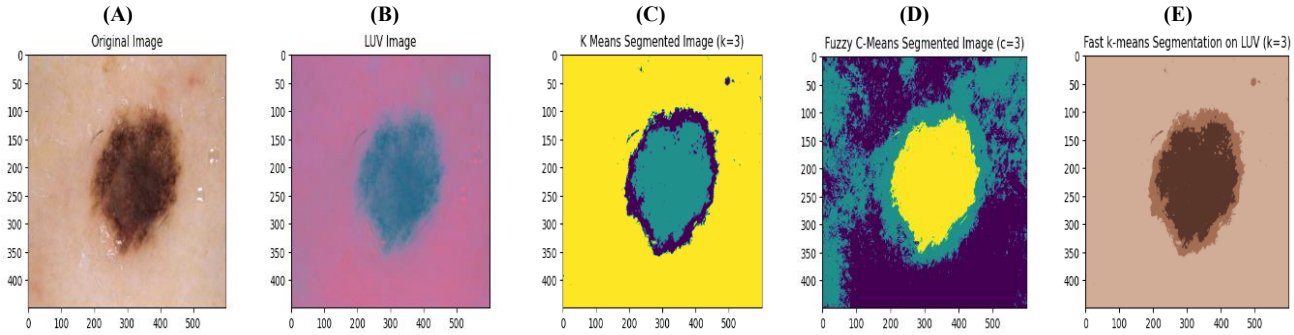


Fig. 2.4: (A) Input# Image Isic_0024319 (B) LUV (C) K-Means (D) FCM (E) FKM.

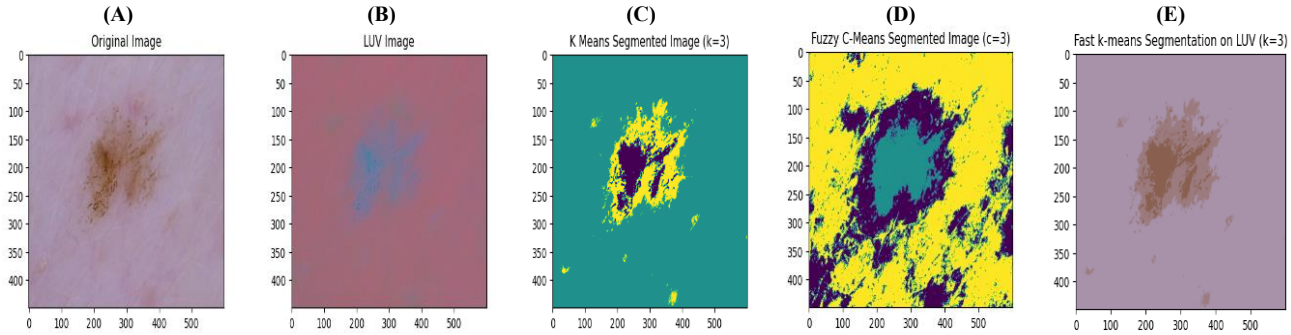


Fig. 2.5: (A) Input# Image ISIC_0024324 (B) LUV (C) K-Means (D) FCM (E) FKM.

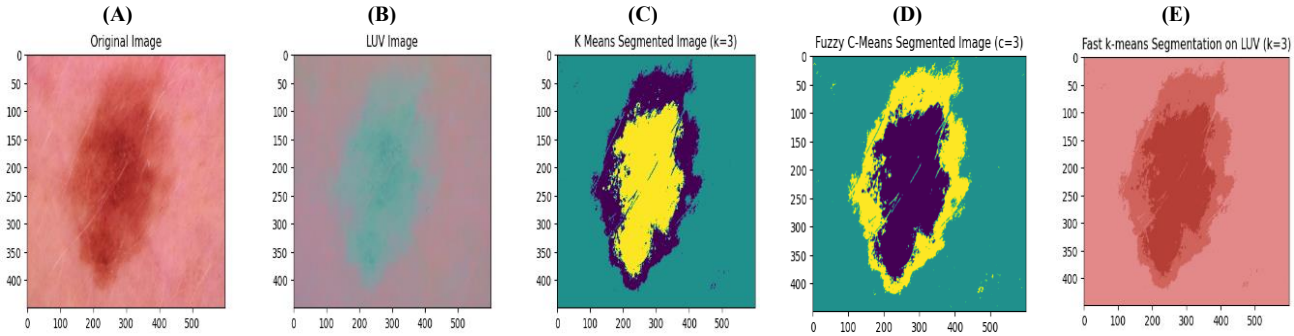


Fig. 2.6: (A) Input# Image ISIC_0024325 (B) LUV (C) K-Means (D) FCM (E) FKM.

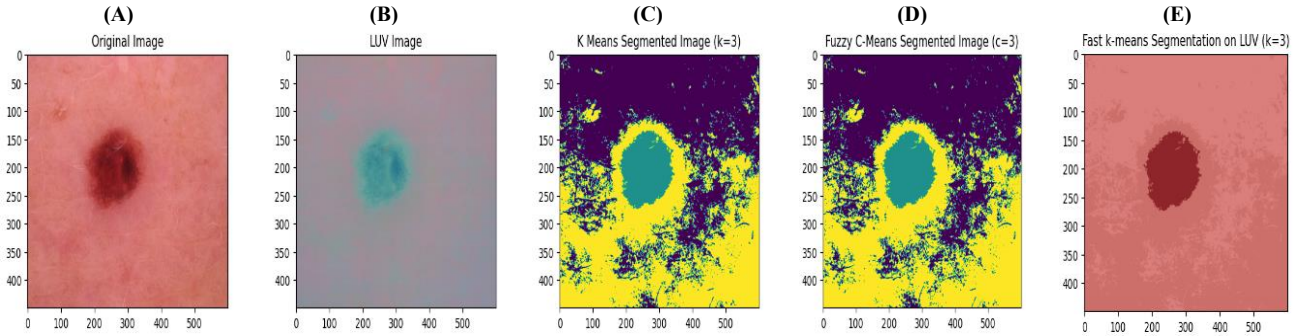


Fig. 2.7: (A) Input# Image ISIC_0024326 (B) LUV (C) K-Means (D) FCM (E) FKM.

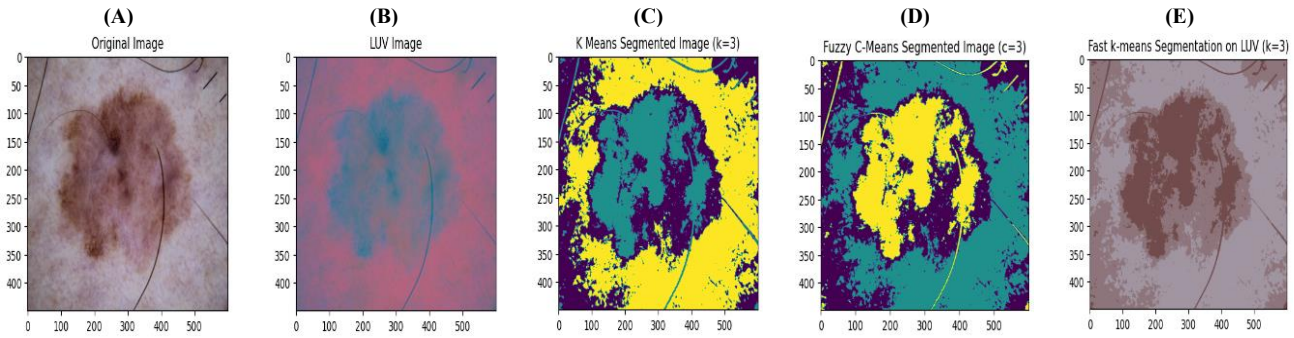


Fig. 2.8: (A) Input# Image ISIC_0024333 (B) LUV (C) K-Means (D) FCM (E) FKM.

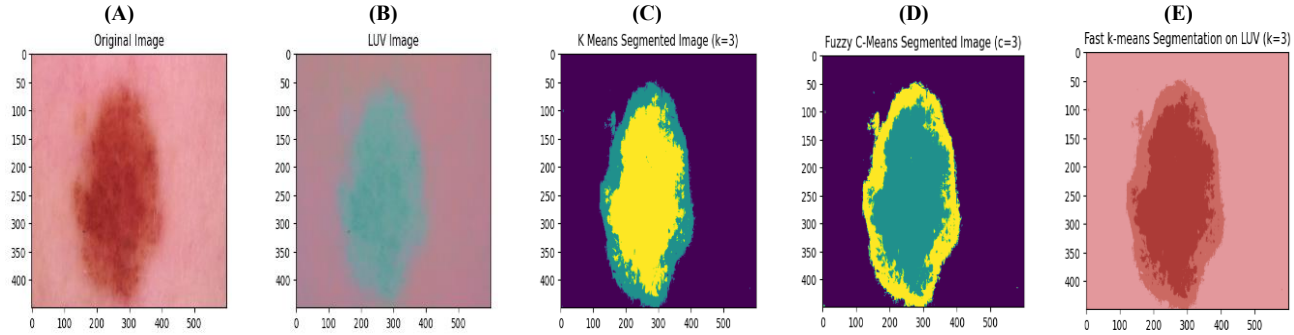


Fig. 2.9: (A) Input# Image ISIC_0024334 (B) LUV (C) K-Means (D) FCM (E) FKM.

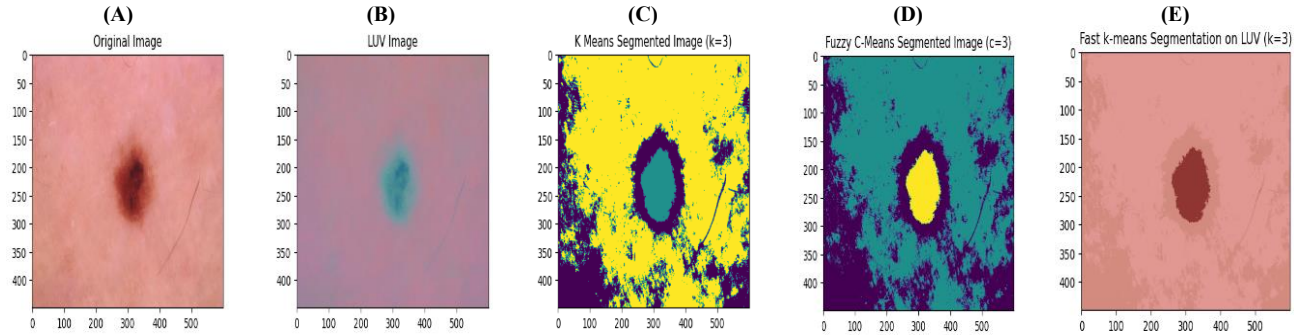


Fig. 2.10: (A) Input# Image ISIC_0024335 (B) LUV (C) K-Means (D) FCM (E) FKM.

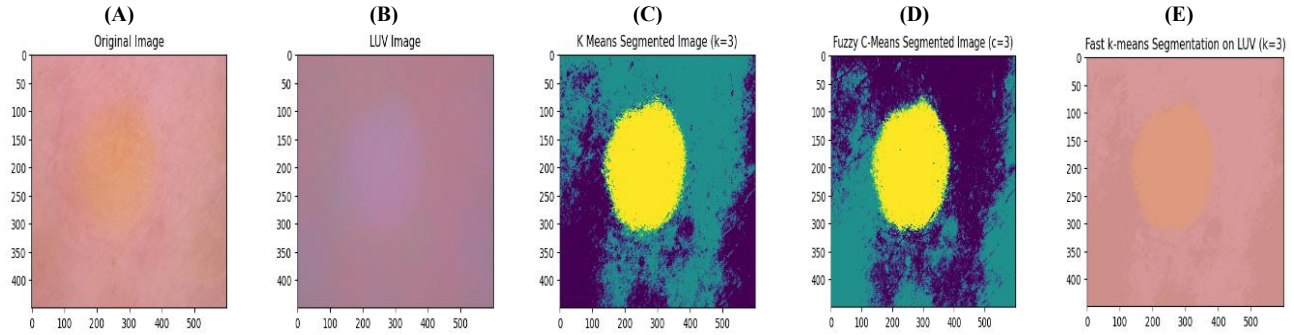


Fig. 2.11: (A) Input# Image ISIC_0024337 (B) LUV (C) K-Means (D) FCM (E) FKM.

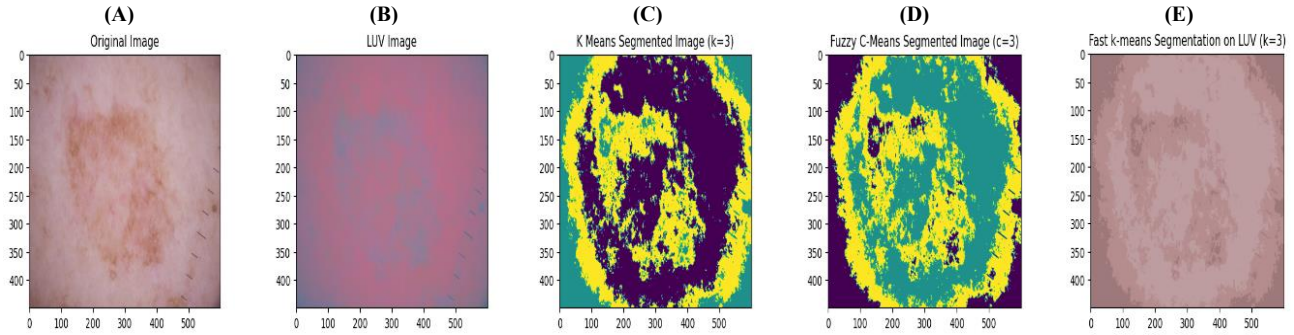


Fig. 2.12: (A) Input# Image ISIC_00243138 (B) LUV (C) K-Means (D) FCM (E) FKM.

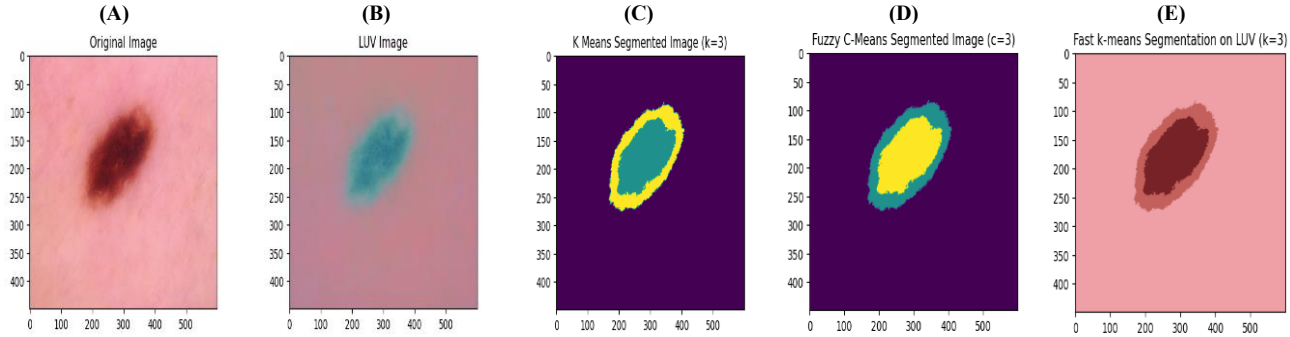


Fig. 2.13: (A) Input# Image ISIC_0024339 (B) LUV (C) K-Means (D) FCM (E) FKM.

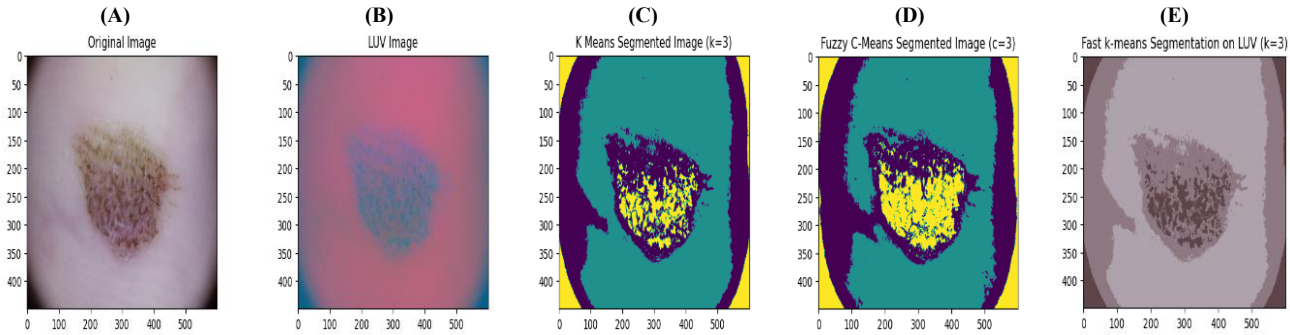


Fig. 2.14: (A) Input# Image ISIC_0024340 (B) LUV (C) K-Means (D) FCM (E) FKM.

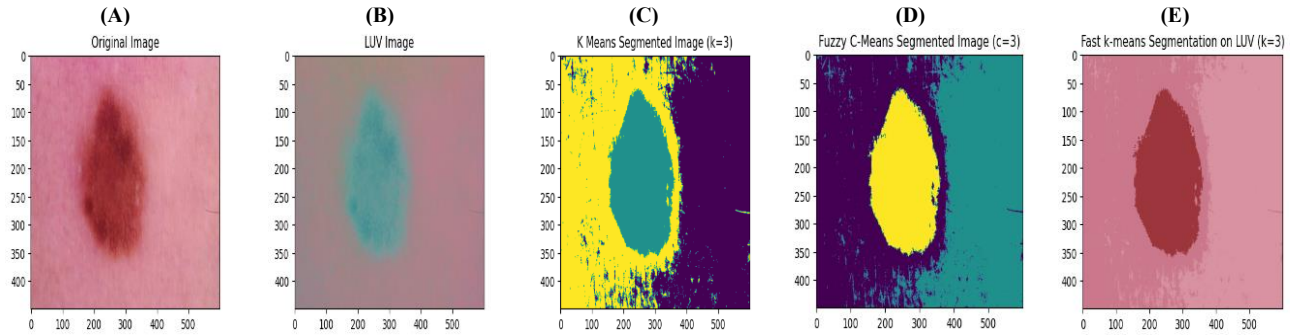


Fig. 2.15: (A) Input# Image ISIC_0024341 (B) LUV (C) K-Means (D) FCM (E) FKM.

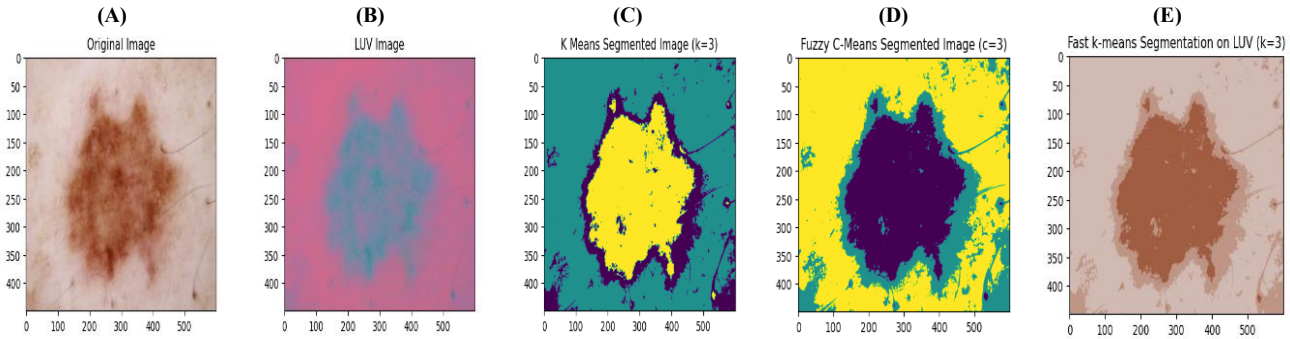


Fig. 2.16: (A) Input# Image ISIC_0024343 (B) LUV (C) K-Means (D) FCM (E) FKM.

The following tables illustrate the outcomes of pixel wise clustered for various methods. As per the ground truth, we state number of clusters is three. Based on this determination the pixels are clustered as three. The normal size of these image is 600 x 450. The total amount of pixels was stated as 2,70,000 as revealed in tables. The Table (Table 1) illustrations the output for K-Means performed on L*u*v based on pixel wise clustered. Table 2 shows the FCM. The proposed method FKM performed on L*u*v has listed in Table 3.

Table 1: Clustered of Pixels for K-Means on L*u*v

IMAGE	CLUSTER 1	CLUSTER2	CLUSTER 3	TOTAL
ISIC 0024315	157790	23686	88524	270000
ISIC 0024317	45673	171608	52719	270000
ISIC 0024318	71957	59358	138685	270000
ISIC 0024319	216656	35995	17349	270000
ISIC 0024320	142531	62698	64771	270000
ISIC 0024321	150654	90086	29260	270000
ISIC 0024322	121851	28731	119418	270000
ISIC 0024323	97772	136946	35282	270000

ISIC 0024324	236440	10820	22740	270000
ISIC 0024325	185851	41995	42154	270000
ISIC 0024326	125292	16041	128667	270000
ISIC 0024327	49224	192926	27850	270000
ISIC 0024330	180343	40510	49147	270000
ISIC 0024331	35845	129526	104629	270000
ISIC 0024332	128982	58039	82979	270000
ISIC 0024333	53948	126073	89979	270000
ISIC 0024334	51378	186669	31953	270000
ISIC 0024335	71433	10080	188487	270000
ISIC 0024336	110457	34647	124896	270000
ISIC 0024337	90329	45157	134514	270000
ISIC 0024338	99631	128786	41583	270000
ISIC 0024339	241076	12986	15938	270000
ISIC 0024340	154025	89404	26571	270000
ISIC 0024341	111928	43775	114297	270000
ISIC 0024342	172546	36644	60810	270000
ISIC 0024343	163115	65667	41218	270000
ISIC 0024344	92259	159166	18575	270000

Table 2: Clustered of Pixels for FCM on L*u*v

IMAGE	CLUSTER 1	CLUSTER 2	CLUSTER 3	TOTAL
ISIC 0024315	94756	23649	151595	270000
ISIC 0024317	46170	171134	52696	270000
ISIC 0024318	134350	59511	76139	270000
ISIC 0024319	97291	130443	42266	270000
ISIC 0024320	67439	139513	63048	270000
ISIC 0024321	129840	34336	105824	270000
ISIC 0024322	28784	118737	122479	270000
ISIC 0024323	49996	97577	122427	270000
ISIC 0024324	71612	22561	175827	270000
ISIC 0024325	44030	183393	42577	270000
ISIC 0024326	15590	127875	126535	270000
ISIC 0024327	49914	28233	191853	270000
ISIC 0024330	62198	58737	149065	270000
ISIC 0024331	42610	123301	104089	270000
ISIC 0024332	58601	125344	86055	270000
ISIC 0024333	56503	93067	120430	270000
ISIC 0024334	32354	52951	184695	270000
ISIC 0024335	9893	94461	165646	270000
ISIC 0024336	120102	114277	35621	270000
ISIC 0024337	128354	96705	44941	270000
ISIC 0024338	49148	117097	103755	270000
ISIC 0024339	13456	240545	15999	270000
ISIC 0024340	94851	41844	133305	270000
ISIC 0024341	113710	113057	43233	270000
ISIC 0024342	157164	70054	42777	270000
ISIC 0024343	53411	68797	147792	270000
ISIC 0024344	18079	151984	99937	270000

Table 3: Clustered of Pixels for Fast K-Means on L*u*v

IMAGE	CLUSTER 1	CLUSTER 2	CLUSTER 3	TOTAL
ISIC 0024315	22694	168289	79017	270000
ISIC 0024317	52534	171779	45687	270000
ISIC 0024318	81101	63684	125215	270000
ISIC 0024319	34244	218807	16949	270000
ISIC 0024320	146110	64052	59838	270000
ISIC 0024321	164758	26704	78538	270000
ISIC 0024322	121133	29288	119579	270000
ISIC 0024323	149247	98740	22013	270000
ISIC 0024324	220127	18026	31847	270000
ISIC 0024325	40708	186878	42414	270000
ISIC 0024326	149301	15590	105109	270000
ISIC 0024327	192278	50028	27694	270000
ISIC 0024330	41801	184695	43504	270000
ISIC 0024331	35011	130697	104292	270000
ISIC 0024332	121119	61758	87123	270000
ISIC 0024333	112400	61846	95754	270000
ISIC 0024334	47573	188736	33691	270000
ISIC 0024335	254318	6612	9070	270000
ISIC 0024336	132177	104988	32835	270000
ISIC 0024337	140352	45255	84393	270000
ISIC 0024338	128876	41570	99554	270000
ISIC 0024339	14628	242600	12772	270000
ISIC 0024340	155092	92671	22237	270000
ISIC 0024341	113745	43852	112403	270000
ISIC 0024342	170167	38460	61373	270000
ISIC 0024343	45135	67915	156950	270000
ISIC 0024344	101644	19518	148838	270000

Table 4: Time Taken (Seconds)

	K MEANS	FUZZY C MEANS	FAST K MEANS
ISIC 0024315	1.9219 s	8.2589 s	2.3210 s
ISIC 0024317	1.7025 s	7.6868 s	1.5503 s
ISIC 0024318	1.9118 s	7.2617 s	2.0585 s
ISIC 0024319	2.7918 s	15.3311 s	2.1715 s
ISIC 0024320	2.0998 s	10.6796 s	1.9009 s
ISIC 0024321	2.2507 s	9.9039 s	1.9332 s
ISIC 0024322	1.7017 s	7.4728 s	1.6340 s
ISIC 0024323	2.4810 s	12.8743 s	2.3821 s
ISIC 0024324	3.1671 s	9.7713 s	3.7718 s
ISIC 0024325	2.1908 s	11.0398 s	1.8450 s
ISIC 0024326	1.6719 s	6.7993 s	1.6917 s
ISIC 0024327	1.8348 s	16.2321 s	2.0512 s
ISIC 0024330	1.9667 s	28.8696 s	2.5834 s
ISIC 0024331	2.1501 s	9.7834 s	2.0537 s
ISIC 0024332	2.0069 s	7.1870 s	1.8094 s
ISIC 0024333	2.2696 s	11.8748 s	2.2673 s
ISIC 0024334	2.4740 s	21.2333 s	2.0306 s
ISIC 0024335	2.3252 s	8.9378 s	2.3048 s
ISIC 0024336	1.9314 s	10.4158 s	1.8458 s
ISIC 0024337	1.6966 s	8.1394 s	1.7473 s
ISIC 0024338	2.0144 s	9.0370	2.0231 s
ISIC 0024339	2.0984 s	11.9329 s	2.0823 s
ISIC 0024340	2.9970 s	16.1121 s	2.8426 s
ISIC 0024341	1.6399 s	4.2024 s	1.5486 s
ISIC 0024342	2.2191 s	16.5794 s	2.1884 s
ISIC 0024343	2.6377 s	24.0142 s	2.6156 s
ISIC 0024344	2.8541 s	14.3842 s	2.9989 s

4. Conclusion

This research work is focused on medical image processing especially skin lesion images. Segregation has performed on these dermoscopic images. Unsupervised algorithm namely Fuzzy C-Means, K-Means and Fast K-Means are performed on various kind of these images. Its take only few seconds for processing. To be crisp, the Fast K-Means method produce the excellent results than others. Despite taking few seconds, Fast K-Means segregate the lesion exactly. Fuzzy C-Means taking more time; however, it leads to over segmentation. K-Means taking less time and produce average results in terms of outcomes. For future enhancement, introduce the hybrid method of optimization technology for segmentation and classifications.

References

[1] AfsahSaleem et al, (2019) "Segmentation and Classification of consumer-grade and dermoscopic skin cancer images using hybrid textural analysis", Journal of Medical Imaging (Bellingham), Aug. Vol 06 (3), https://doi.org/10.1117/1.JMI.6.3.039802.

[2] Ananth Sivaprakasam, V.Saravanakumar et al, (2018), "Wavelet based cervical image segmentation using morphological and statistical Operations", Journal of Advanced Research in Dynamical & Control Systems, Vol. 10-03, http://www.jardcs.org/abstract.php?archiveid=3838.

[3] Dey, N.; Rajinikanth, V.; Ashour, A.S.; Tavares, J.M.R.S, (2018), "Social Group Optimization Supported Segmentation and Evaluation of Skin Melanoma Images". *Symmetry*, *10*, 51. https://doi.org/10.3390/sym10020051.

[4] Huang, L., Zhao, Y. & Yang, T, (2019), "Skin lesion segmentation using object scale-oriented fully convolutional neural networks", SIViP 13, 431–438. https://doi.org/10.1007/s11760-018-01410-3

[5] M.Kavitha, Tzung-Pei Hong et al., (2022), "Fuzzy Clustering Technique For Segmentation On Skin Cancer Dermoscopic Images", Fuzzy Mathematical Analysis and Advances in Computational Mathematics, part of the Studies in Fuzziness and Soft Computing" Vol 419, Page 81-89, https://link.springer.com/chapter/10.1007/978-981-19-0471-4_6 . https://doi.org/10.1007/978-981-19-0471-4_6.

[6] Ning Wang et al., (2018), "Skin Lesion image segmentation based on adversarial networks", KSII Transactions on Internet and Information Systems Vol. 12, No. 6, Jun., 2826 https://doi.org/10.3837/tiis.2018.06.021.

[7] Oludayo O et.al, (2018) "Segmentation of melanoma skin lesion using perceptual colour difference saliency with morphological analysis", Hindawi – Mathematical problems in Engineering, Feb, https://doi.org/10.1155/2018/1524286

[8] Skin Cancer Prevention Progress Report (2017), Atlanta, GA: Centers for Disease Control and Prevention, US Dept of Health and Human Services. https://www.cdc.gov/cancer/skin/pdf/SkinCancerPreventionProgressReport_2017.pdf.

[9] Sudhakar Singh, Masood Alam & Bharat Singh (2020) Orthogonal moment feature extraction and classification of melanoma images, Journal of Information and Optimization Sciences, 41:1, 195-203, https://doi.org/10.1080/02522667.2020.1721585

[10] SudhritiSenqupta, Neetu Mittal and MeghaModi, (2020), "Improved skin lesion detection using color space and artificial intelligence techniques", Journal of Dermotological Treatment, https://doi.org/10.1080/09546634.2019.1708239.

[11] Bavya S, Saravana Kumar. V, Kavitha M and Anantha Sivaprakasam, (2024), "Segmentation of Skin Lesion Image Using FCM with Color Transformation Saliency," *2024 IEEE International Conference on Computing and Data Science (ICCDS)*, Chennai, India, June 2024, pp. 1-6, https://doi.org/10.1109/ICCDS60734.2024.10560421.

[12] V.Saravana Kumar and E.R.Naganathan, (2018), "Hyperspectral Image Segmentation Based on Enhanced Estimation of Centroid with Fast K-Means", International Arab Journal of Information Technology, Jordon, Vol.15, no 5, pp- 904-911, Sep, https://iajit.org/PDF/September%202018,%20No.%205/10400.pdf